Investigating flow-barrier impact mechanisms using two soil types in centrifuge tests

S. Cuomo, A. Di Perna, M. Moscariello, R. Ciaglia
Geotechnical Engineering Group (GEG), University of Salerno, Italy,
scuomo@unisa.it, angeladipernaadp@gmail.com, mamoscariello@unisa.it, rciaglia@unisa.it

M. Martinelli
SPERI spa, Roma, Italy; former Deltares, Delft, Netherlands, Mario.martinelli@hotmail.it

N. Nappo, J.H.A. Langstraat, F. Kop, S.J.M. van Eekelen
Deltares, Delft, Netherlands, nicoletta.nappo@deltares.nl,
john.langstraat@deltares.nl, fransenhennykop@gmail.com, suzanne.vaneekelen@deltares.nl

ABSTRACT: Propagation-impact experiments were conducted in a beam centrifuge at 40*g*-level. A saturated soil mass was released, propagated along an instrumented slope, and finally impacted against a barrier. The tests performed against a fixed steel barrier provide a baseline for understanding the influence of soil type on impact forces and interaction mechanism. A significant finding emerges from the comparison between the two soil types: the peak impact pressure measured directly on the rigid barrier is consistently higher for the uniform Baskarp sand compared to a finer-grained poorly graded volcanic natural soil. This suggests that the grain size distribution plays a direct role in the mechanism of stress transmission upon impact against a rigid structure.

1 INTRODUCTION

Protection barriers are an important option to mitigate the risk posed by flow-like landslides (Cascini et al., 2010). However, the hydromechanical interaction between flowing masses and a barrier is governed by multiple factors, with particle size distribution playing a critical role in controlling impact pressures (Jiang et al., 2015; Song et al., 2017; Cui et al., 2018).

While theoretical frameworks classify landslide-structure interaction (LSI) mechanisms based on dimensionless parameters (for instance, Faug et al., 2015), studies with materials of different grain size distributions remain limited. On the other hand, most experimental studies use uniform materials that do not represent the complex, natural soils typically involved in flowslides.

This paper presents an experimental investigation using centrifuge tests under 40*g*. Two materials are employed for impact tests against fixed rigid barriers. Eight tests covering two barrier positions and two released masses enable the isolation of grain-size distribution effects on impact pressures and flow kinematics. High-speed imagery and load cell measurements offer a comprehensive characterization within Faug's (2015) framework.

2 MATERIALS AND METHODS

The experimental campaign employed two materials selected to investigate the influence of grain size distribution on flow-barrier interaction: Baskarp B25 sand, a uniform silica sand; and a natural, poorly-graded, volcanic silty-sand, previously classified in literature as "Ashy B soil" (Cuomo et al., 2010, 2014), sampled from the Sarno site (Southern Italy), where catastrophic landslides occur (Cascini et al., 2008).

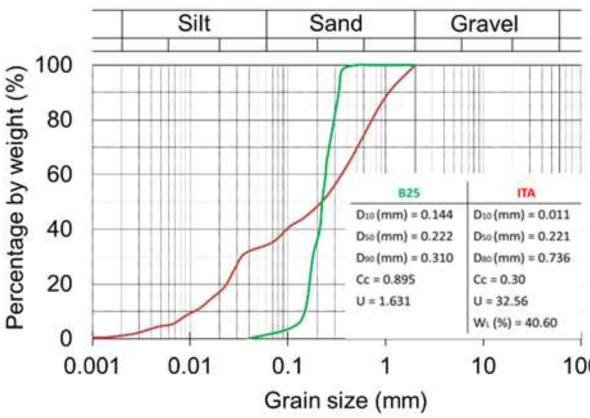

Figure 1. Grain-size distribution and relevant features of the soil types used in the centrifuge tests.

Baskarp B25 Sand is a Swedish silica sand with specific gravity Gs = 2.65, widely used as a reference material in geotechnical research due to its well-characterized properties and high uniformity. The grain size distribution (Figure 1, green curve) is tightly constrained within the sand fraction: D_{10} = 0.144 mm, D_{50} = 0.222 mm, and D_{90} = 0.310 mm. The resulting uniformity coefficient U = D_{60}/D_{10} = 1.631 and coefficient of curvature Cc = 0.895 confirm the nearly uniform nature of this material. The narrow grain size range (spanning approximately 0.14-0.31 mm) results in a well-sorted fabric with predominantly sand-to-sand contacts and relatively large, interconnected pore spaces.

ITA soil is a natural pyroclastic soil with specific gravity Gs = 2.65. The grain size distribution (Figure 1, red curve) spans nearly three orders of magnitude: D_{10} = 0.011 mm (fine silt), D_{50} = 0.221 mm (medium sand), and D_{80} = 0.736 mm (coarse sand). This wide gradation yields a very high uniformity coefficient U = 32.56 and a low coefficient of curvature Cc = 0.30, characteristic of poorly-graded soils. The material composition includes approximately 30-35% silt-sized particles (< 0.063 mm) and 65-70% sand (0.063-2 mm). The fine fraction exhibits moderate plasticity, with liquid limit wL = 40.60%.

The tests were conducted at the Deltares Geotechnical Centrifuge (Figure 2) at N = 40g (Cuomo et al., 2024). Details on the experimental setup, instrumentation, and testing procedures are provided in Cuomo et al. (2024, 2026a-b).

Fixed rigid steel barriers (height H = 100 mm, width = 200 mm) are positioned at two locations (Figure 3): "near" (66 mm from slope toe) and "far" (266 mm from slope toe), at the model scale.

Figure 2. Side view of the beam GeoCentrifuge of Deltares.

To satisfy centrifuge scaling laws, soils are saturated with CMC solution (μ = 0.04 Pa·s at 40g, equivalent to water viscosity at prototype scale) following established procedures for dynamic centrifuge modeling (Adamidis & Madabhushi, 2015). Samples are prepared 12 hours before testing and continuously mixed during spin-up to prevent segregation.

Two released masses (7.5 kg and 10.5 kg) are tested for each material-position combination. Kyowa BED-A-1MP pressure transducers (>1000 Hz sampling) measure impact pressures, while high-speed cameras (2500 fps) record flow kinematics. Eight tests are conducted: 4 with B25 sand (Tests 02, 04, 12, 16) and 4 with ITA soil (Tests 03, 05, 13, 17) against fixed barriers.

Flow thickness (h*) and velocity (v*) are extracted from high-speed imagery following a systematic procedure based on two temporal references (Figure 4): t_0, the initial instant when the flow is clearly recognizable several frames before impact, and t_1, the impact instant corresponding to the first contact between the flow front and the barrier.

Flow thickness measurements are performed at both instants using FIJI image processing software, with distances h_0 and h_1 measured perpendicular to the slope surface. The reference flow thickness is calculated as the arithmetic mean:

$$h^* = \frac{(h_0 + h_1)}{2} \quad (1)$$

accounting for gradual deceleration as the flow approaches the barrier. The uncertainty on h* is estimated as:

$$\Delta h^* = \frac{(h_1 - h_0)}{2} \quad (2)$$

representing the semi-range of thickness variation between the two temporal references.

Flow velocity is determined from the spatial displacement Δs of a recognizable flow feature (typically the flow front) divided by the time interval:

$$\Delta t = t_1 - t_0 \quad (3)$$

$$v^* = \frac{\Delta s}{\Delta t} \quad (4)$$

The uncertainty on velocity, derived from error propagation considerations on spatial measurement, is estimated as:

$$\Delta v = \sqrt{2} \cdot \frac{\Delta s}{\Delta t} \quad (5)$$

The Froude number:

$$F_r = \frac{v^*}{\sqrt{g \cdot h^*}} \quad (6)$$

where g is the gravitational acceleration at centrifuge scale ($N \cdot g$ = 40·9.81 m/s²), and the barrier-to-flow height ratio H/h* (where H = 0.10 m) provides dimensionless parameters for classifying interaction mechanisms within Faug's (2015) framework.

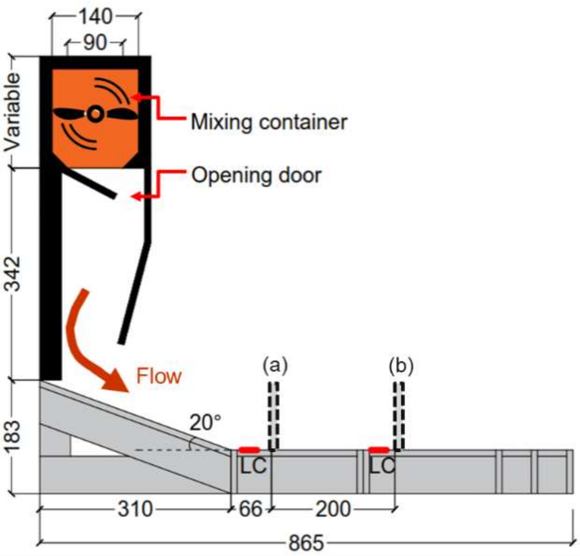

Figure 3. Configuration of experiments with fixed barriers at (a) near and (b) far positions used to infer the reference value of h and v* for Test 16.*

3 RESULTS

High-speed imagery analysis enables the extraction of flow thickness (h^*) and velocity (v^*) at a reference instant immediately before the flow touches the barrier for all eight tests (Figure 4).

For B25 sand, flow velocities range from 7.3 m/s (Test 04, far barrier, mass of 7.5 kg) to 13.6 m/s (Test 16, near barrier, mass of 10.5 kg), with flow depths between 0.016 m and 0.044 m, at the model scale.

ITA soil exhibits slightly lower velocities under comparable conditions, ranging from 7.3 m/s (Test 05, far barrier, mass of 7.5 kg) to 11.3 m/s (Test 17, near barrier, mass of 10.5 kg), with flow depths of 0.017-0.028 m.

The generally thinner flows observed with ITA soil, despite similar released masses, suggest enhanced flow spreading during propagation, likely facilitated by the fine fraction and higher pore fluid content.

The resulting Froude numbers span from 2.21 (Test 12, B25, far barrier, mass of 7.5 kg) to 4.58 (Test 13, ITA, near barrier, mass of 10.5 kg) for the eight fixed barrier tests. The barrier-to-flow height ratio H/h* varies from 1.77 (Test 04, B25, thick flow) to approximately 5.9 (Test 13, ITA, thin flow). Uncertainties in Fr range from ±0.02 to ±0.60, while uncertainties on H/h^* range from ±0.5 to ±1.2, reflecting the natural variability in flow thickness measurement.

Figure 4. Example of images of the incoming flow (Test 16).

Figure 5 represents all experimental tests within Faug's (2015) interaction mechanism diagram, with all data points falling in the standing jump region as confirmed by observations from high-speed imagery.

Qualitative differences between the two materials are observed during the interaction phase. Flows with B25 sand exhibit more abrupt deceleration with concentrated vertical run-up and rapid material consolidation immediately behind the barrier.

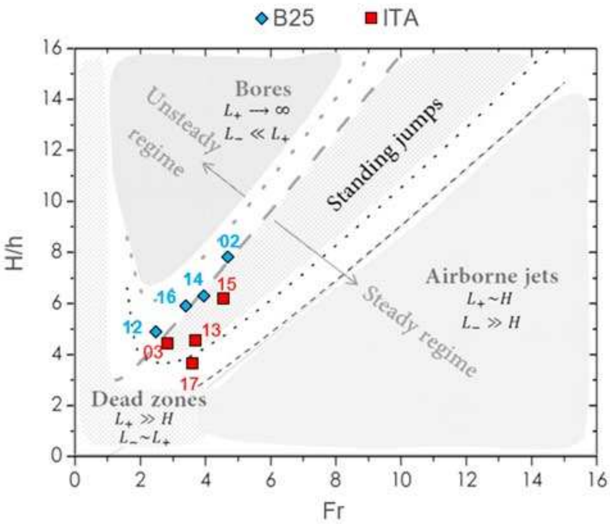

Figure 5. Kinematic features of the incoming flow and expected interaction mechanisms for all the tests of Table 1. H/h and Fr plotted are the average values, with

uncertainty varying for each test from a minimum of +-0.02 and a maximum of 0.60 concerning the Froude number, and a minimum of +-0.5 and a maximum of +-1.2 as for the H/h ratio.

In contrast, flows with ITA soil show more gradual deceleration, distributed run-up with lateral spreading along the barrier face, and prolonged material deposition requiring a longer time to consolidate behind the barrier. More investigations are needed (Cuomo et al., 2026a, 2026b) also based on extended interpretation of experimental results and enhanced numerical modelling.

4 CONCLUSIONS

This study investigates the influence of grain size distribution on flow-barrier interaction through centrifuge testing at *40g*. Uniform Baskarp B25 sand and natural poorly graded ITA volcanic silty-sand were tested against fixed rigid barriers under identical conditions.

The tests for both materials fall within the standing jump regime according to Faug's (2015) classification. However, qualitative differences emerge: B25 sand exhibits abrupt deceleration and concentrated run-up with immediate consolidation, while ITA soil shows gradual deceleration, distributed run-up with pronounced spreading, and prolonged consolidation time.

These observations show that grain size distribution influences detailed interaction mechanisms, even within the same general regime. Understanding material-dependent impact behavior is important for designing mitigation structures in volcanic regions where poorly graded natural soils are prevalent, and further tests are desirable for enhanced understanding.

ACKNOWLEDGEMENTS

The authors are grateful for the financial support provided the European Union's Horizon 2020 research and innovation program under Grant Agreement No. 101006512 for the transnational GEOLAB project FIM. The research was also supported by the Project FARB 2021 "Greened Protection Structures against flow-like landslides" of the University of Salerno (Italy) and by Geosintex s.r.l. (Italy).

REFERENCES

Adamidis, O., & Madabhushi, S. P. G. (2015). Use of viscous pore fluids in dynamic centrifuge modelling. International Journal of Physical Modelling in *Geotechnics*, 15(3), 141-149.

Cascini, L., Cuomo, S., & Guida, D. (2008). Typical source areas of May 1998 flow-like mass movements in the Campania region, Southern Italy. *Engineering Geology*, 96(3-4), 107-125

Cascini, L., Cuomo, S., Pastor, M., & Sorbino, G. (2010). Modeling of rainfall-induced shallow landslides of the flow-type. *Journal of Geotechnical and Geoenvironmental Engineering*, 136(1), 85-98.

Choi, C. E., Au-Yeung, S. C. H., Ng, C. W. W., & Song, D. (2015). Flume investigation of landslide granular debris and water runup mechanisms. *Géotechnique Letters*, 5(1), 28-32.

Cuomo, S., Pastor, M., Cascini, L., & Castorino, G. C. (2014). Interplay of rheology and entrainment in debris avalanches: a numerical study. *Canadian Geotechnical Journal*, 51(11), 1318-1330.

Cuomo, S., Di Perna, A., Moscariello, M., Martinelli, M., Nappo, N., Langstraat, J. H. A., Kop, F. S. J. M., & van Eekelen, S. J. M. (2024). Flowslide Impact Modelling (FIM) project: centrifuge tests. *Proceedings of ECPMG 2024; 5th European Conference on Physical Modelling in Geotechnics* 2-4 October 2024, Delft, the Netherlands, (https://www.issmge.org/uploads/publications/53/125/ECPMG2024-65.pdf, accessed on 19 June 2025).

Cuomo, S., Di Perna, A., Ciaglia, R., Moscariello, M., & Martinelli, M. (2026a). Impact of flow-like landslide on protection barrier: Centrifuge Tests and MPM modelling. *Engineering Geology*.

Cuomo, S., Di Perna, A., Ciaglia, R., Moscariello, M., & Martinelli, M. (2026b). Interaction of flowslides with fixed and mobile barriers: centrifuge tests on Baskarp and Vesuvian soils. *Canadian Geotechnical Journal*.

Faug, T. (2015). Depth-averaged analytic solutions for free-surface granular flows impacting rigid walls down inclines. Physical Review E, 92(6), 062310.

Jiang, Y. J., Zhao, Y., Towhata, I., and Liu, D. X. (2015). Influence of particle characteristics on impact event of dry granular flow. Powder Technology, 270, 53-67.

Moscariello, M., Cuomo, S., Baumann, V., & Bonadonna, C. (2021). On the features of pyroclastic deposits and post-eruption natural hazards. In *Geohazard Mitigation: Select Proceedings of VCDRR 2021* (pp. 157-170). Singapore: Springer Singapore.

Song, D., Ng, C. W. W., Choi, C. E., Zhou, G. G., Kwan, J. S., & Koo, R. C. H. (2017). Influence of debris flow solid fraction on rigid barrier impact. *Canadian Geotechnical Journal*, 54(10), 1421-1434.